

# Expression of an archaeal chaperonin in *E. coli*: formation of homo- ( $\alpha$ , $\beta$ ) and hetero-oligomeric ( $\alpha + \beta$ ) thermosome complexes

Thomas Waldmann, Michael Nitsch, Martin Klumpp, Wolfgang Baumeister\*

Max Planck Institut für Biochemie, Am Klopferspitz 18a, 82152 Martinsried, Germany

Received 19 October 1995

**Abstract** Co-expression of the two genes encoding the  $\alpha$ - and  $\beta$ -subunit of the *Thermoplasma acidophilum* thermosome in *Escherichia coli* yielded fully assembled hetero-oligomeric complexes ( $\alpha + \beta$ ). Surprisingly, also separate expression of both genes resulted in formation of hexadecameric complexes ( $\alpha$ ,  $\beta$ ) in the bacterial cytoplasm. On electron micrographs these complexes were indistinguishable from each other and from the native thermosome. The recombinant  $\alpha$ -complex as well as the native thermosome could be reconstituted in vitro from their dissociated subunits in the presence of Mg-ATP.

**Key words:** Thermosome; Molecular chaperone; Gene expression; Archaeobacteria; *Thermoplasma acidophilum*; Electron microscopy

## 1. Introduction

Chaperonins, a major class of molecular chaperones [1–3], play an important role in the cellular folding of nascent or non-native polypeptides. These high molecular mass ATPases ( $M_r \sim 1 \times 10^6$ ) are formed by either one or several different but related protein-subunits ( $M_r \sim 60,000$ ) which assemble into toroidal complexes consisting of two stacked 7–9-membered rings. Two chaperonin-families of distant evolutionary relationship have been characterized [4,5] and were recently classified as group I and group II [6]. Group I chaperonins comprise the highly conserved GroEL-like complexes found in eubacteria, mitochondria and chloroplasts whereas group II encompasses the cytosolic chaperonins of eukaryotes (known as TRiC [7] or CCT [8]) and archaeobacteria (the thermosome [9], also named TF55/TF56 [10, GenBank accession number L4691]). Whereas all members of group I are tetradecameric complexes built by one or two different subunits, the group II chaperonins are more heterogeneous regarding the subunit composition and the rotational symmetry of the toroids. TRiC is composed of at least eight types of polypeptides which assemble into pseudo eight-fold symmetric complexes [11,12]. In contrast, the thermosome consists of only two different subunits which form eight-fold (*Pyrodicticum occultum*, *Thermoplasma*

*acidophilum*) [12,13] or ninefold symmetric rings (*Sulfolobus* sp.) [10,14].

A three-dimensional reconstruction of the *Pyrodicticum occultum* thermosome from electron micrographs revealed a kidney-shape of the subunits apparently formed by two terminal domains interconnected by a smaller central domain [13]. Recently, the primary structure of both thermosome-subunits from *Thermoplasma acidophilum* was obtained by cloning and sequencing of the corresponding genes [15]. Sequence alignments with other group I and group II chaperonins revealed a three-domain architecture [15,16] corresponding to the equatorial, intermediate and apical domain which were identified in the crystal structure of GroEL from *E. coli* [17].

The thermosome of *T. acidophilum* appears to contain both subunits in equal amounts [12]. So far, it was not possible to decide whether both polypeptides form separate eight-membered rings or alternate within each ring of the complex. We expressed in *E. coli* the genes for the  $\alpha$ - and  $\beta$ -subunit jointly and separately and isolated different ring-shaped thermosome-like complexes apparently consisting of only the  $\alpha$  or  $\beta$  or of  $\alpha + \beta$  polypeptides. For the native thermosome and likewise for the  $\alpha$ -complex we have shown that it can be dissociated and reassembled in vitro. We anticipate that, as in the case of the proteasome, another high molecular mass complex from *T. acidophilum* [18–21], the expression of functional complexes in an *E. coli* system provides a basis for addressing important issues regarding the assembly pathway or function. The relative simplicity of the thermosome compared with the eukaryotic CCT or TRiC greatly facilitates such experiments.

## 2. Materials and methods

Unless otherwise specified, molecular biology reagents were purchased from New England Biolabs, other chemicals from Sigma or Merck in the highest quality grade available. Standard molecular biology techniques were performed according to Sambrook et al. [22].

### 2.1. Cloning of the $\alpha$ - and $\beta$ -gene into the expression vectors

The expression vectors pT7-5, pT7-7 [23] and pRSet 6a [24], which all contain the pT7-promotor followed by a *E. coli* Shine-Dalgarno sequence (not pT7-5) and a polylinker-region, were used for separate and co-expression of the thermosome-subunits. The reading frames for the two subunits were amplified by polymerase chain reaction (PCR) using two pUC 18 clones as templates, which harbour either the *thiA* gene for the  $\alpha$ - or the *thiB* gene for the  $\beta$ -subunit on a *Hind*III-fragment [15]. Various non-degenerated primer pairs (26–52-mers) were designed in order to introduce flanking 5'- and 3'-restriction-sites corresponding to the respective polylinkers of the used expression vector. In addition, a Shine-Dalgarno sequence preceding the  $\beta$ -gene and 6 additional C-terminal histidine residues (indicated as (6 His)) in the  $\alpha$ - or  $\beta$ -reading frame were facultatively inserted. PCR was performed with a Perkin-Elmer Cetus 480 thermocycler using the heat-stable polymerase *Pfu*

\*Corresponding author. Fax: (49) (89) 8578-2641.

**Abbreviations:** AMPPNP, 5'-adenylylimido-diphosphate; ATP $\gamma$ S, adenosine 5'-O-(3-thiotriphosphate); CCT, chaperonin containing TCP-1; IPTG, isopropyl- $\beta$ -D-thiogalactopyranoside; OD<sub>600</sub>, optical density measured at 600 nm; PCR, polymerase chain reaction; pI, isoelectric point; PMSF, phenylmethanesulfonyl fluoride; TF55/56, thermophilic factor of 55/56 kDa; TRiC, TCP-1 ring complex.

isolated from *Pyrococcus furiosus* (Stratagene). For separate expression the  $\alpha$ -gene was cloned into pRSet 6a or pT7-7 using a 5'-*Nde*I and a 3'-*Eco*RI site whereas the  $\beta$ -gene was cloned in pT7-5 using a 5'-*Sal*I and a 3'-*Hind*III site due to several *Nde*I sites occurring within the  $\beta$ -gene. For co-expression of both polypeptides the  $\beta$ -gene was cloned into pRSet 6a- $\alpha$  using *Kpn*I and *Pst*I or pT7-7- $\alpha$  using *Sal*I and *Hind*III. The His-tag was appended either to the  $\alpha$  or  $\beta$  polypeptide. Fig. 1 shows schematically the different expression constructs, named pRSet 6a- $\alpha$ (6 His), pT7-5- $\beta$ (6 His) and pRSet 6a- $\alpha$ - $\beta$ (6 His). The integrity of the reading frames was confirmed by DNA sequencing on 373A DNA sequencer using a Dye Deoxy Terminator Cycle sequencing kit (Applied Biosystems).

## 2.2. Expression and purification of the recombinant protein complexes

For screening and propagation of plasmids we used *E. coli* XL1-blue (Stratagene); the expression was performed in *E. coli* BL21(DE3) cells, which contain the T7 RNA-polymerase gene included in their genome under the control of a lacUV5 promoter [25]. The expression vectors were transformed by electroporation in a *E. coli* Pulser (Bio-Rad). Cells were grown in LB-medium (100  $\mu$ g ampicillin/ml) to an OD<sub>600</sub> of 0.8–1 at 37°C and induced with 1 mM isopropyl- $\beta$ -D-thiogalactopyranoside (IPTG) for 4 h. After harvesting the cells by centrifugation, the pellet was frozen and thawed, resuspended in 50 mM sodium phosphate buffer, pH 7.5, 150 mM NaCl, 1 mM phenylmethanesulfonyl fluoride (PMSF), 5% (v/v) glycerol. The cells were lysed by sonication (four times for 30 s) and centrifuged at 100,000  $\times$  g for 30 min at 4°C. For Ni<sup>2+</sup>-chelate affinity chromatography on a Fractogel EMD Chelate column (Merck) at 4°C the supernatant was diluted twofold with the column-equilibration buffer (20 mM sodium phosphate, 0.5 M NaCl, 1 mM imidazole, pH 7.0) and applied to the column (8  $\times$  1.5 cm). Proteins were eluted with a 30 ml gradient of 1–500 mM imidazole in the equilibration buffer. Fractions containing the expected protein were pooled, concentrated by ultrafiltration in Centrprep 10 and Centricon 30 columns (Amicon) and loaded on a Superose 6 gel filtration column running at room temperature in Tris-HCl, pH 7.5, 150 mM NaCl, 1 mM EDTA, 5% (v/v) glycerol (Buffer A) at a flow rate of 0.5 ml/min. Purification was monitored by Tricine-SDS-PAGE (10% polyacrylamide) and non-denaturing PAGE (3–10% polyacrylamide gradient gels) followed by Coomassie blue staining [12] or by Western blot analysis. For immuno-staining the polyacrylamide gels were blotted

onto nitrocellulose and probed with an polyclonal rabbit antiserum against purified thermosomes from *Pyrodicticum occultum* (kindly provided by A. Hoffmann and K.O. Stetter, Regensburg) [9]. N-Terminal sequences of the expressed polypeptides were obtained by Edman-degradation.

## 2.3. Electron microscopy and image analysis

For electron microscopy aliquots of purified protein solutions were applied to carbon-coated copper grids and negatively stained with 2% uranyl acetate. Images were recorded at a magnification of 33,600 $\times$  under low-dose conditions, using a Philips CM12 electron microscope. Non-overlapping areas of micrographs were digitized using an Eikonix 1412 camera system at a pixel size of 15 nm, corresponding to 0.45 nm at the specimen level. For image analysis, pictures were band-pass filtered in Fourier space within the space frequency limits of 0.625 nm<sup>-1</sup> and 0.05 nm<sup>-1</sup>. The alignment of side-views via cross correlation was performed with the help of an arbitrarily chosen reference in an iterative way and using the SEMPER image processing software package [26]. For the image analysis of the ring-shaped end-on views a method based on eigenvector-eigenvalue data analysis was used as described elsewhere [14].

## 2.4. In vitro dissociation and reassembly

The thermosomes from *T. acidophilum* were purified as described in [12]. Fractions containing the thermosome (1.5 mg/ml in 20 mM Tris-HCl, 150 mM NaCl, 1 mM DTT, 5 mM NaN<sub>3</sub> and approximately 20% (v/v) glycerol) or the  $\alpha$ -complex (in buffer A as purified from *E. coli*) were diluted to a protein concentration of 0.55 mg/ml with 20 mM Tris-HCl, pH 7.5. In order to dissociate the hexadecameric complexes, 10% (v/v) of 1 M glycine-HCl, pH 3, was added resulting in a protein concentration of 0.5 mg/ml, a glycerol concentration of  $\leq$  5% (v/v) and a glycine concentration of 100 mM. After a 3 h incubation period, aliquots of 25  $\mu$ l of the dissociation mixture were dialyzed overnight in a microdialysis apparatus as described by Lissin [27] against 2 ml of 50 mM Tris-HCl, pH 6.8, 20% (v/v) glycerol, 1 mM DTT plus, optionally, 20 mM KCl, 10 mM MgOAc<sub>2</sub> and 1 mM ATP, ADP, ATP $\gamma$ S or AMPNP as specified. All experiments were performed at room temperature. 20  $\mu$ l of the dialysate was applied to a non-denaturing polyacrylamide gel, the remainder was used for examination by electron microscopy.

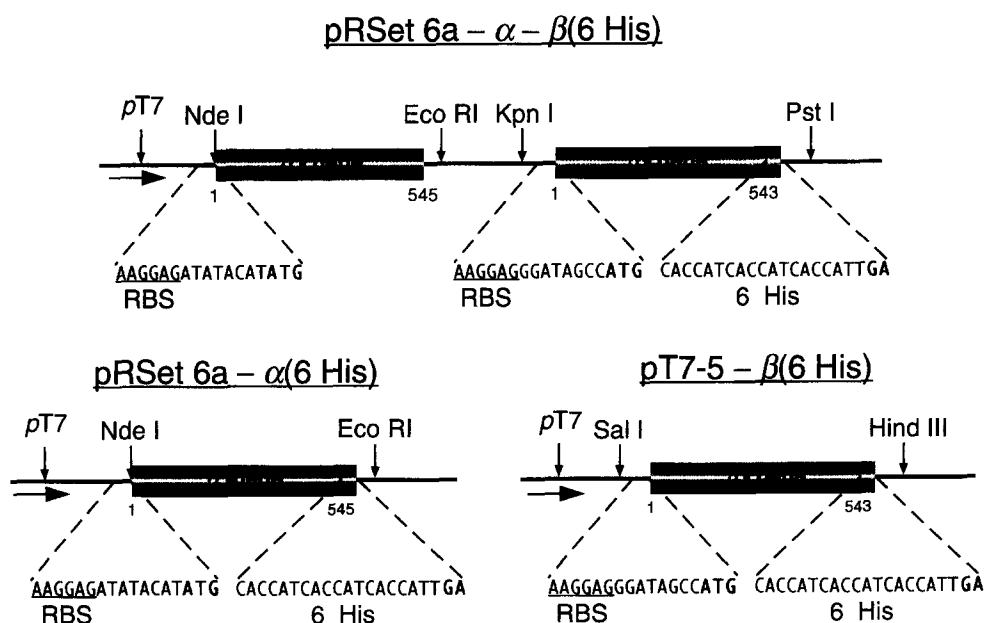


Fig. 1. Schematic drawing of the expression constructs pRSet 6a- $\alpha$ - $\beta$ (6 His), pRSet 6a- $\alpha$ (6 His) and pT7-5- $\beta$ (6 His) used for separate and co-expression of the genes encoding the thermosome-subunits. Restriction sites for cloning are indicated by vertical arrows. Direction of transcription starting from the T7-promotor (pT7) is indicated by horizontal arrows. Nucleotide sequences are given for the ribosomal binding site (RBS, underlined) and the His-tag (6 His); start and termination codons are printed in bold type letters, respectively.

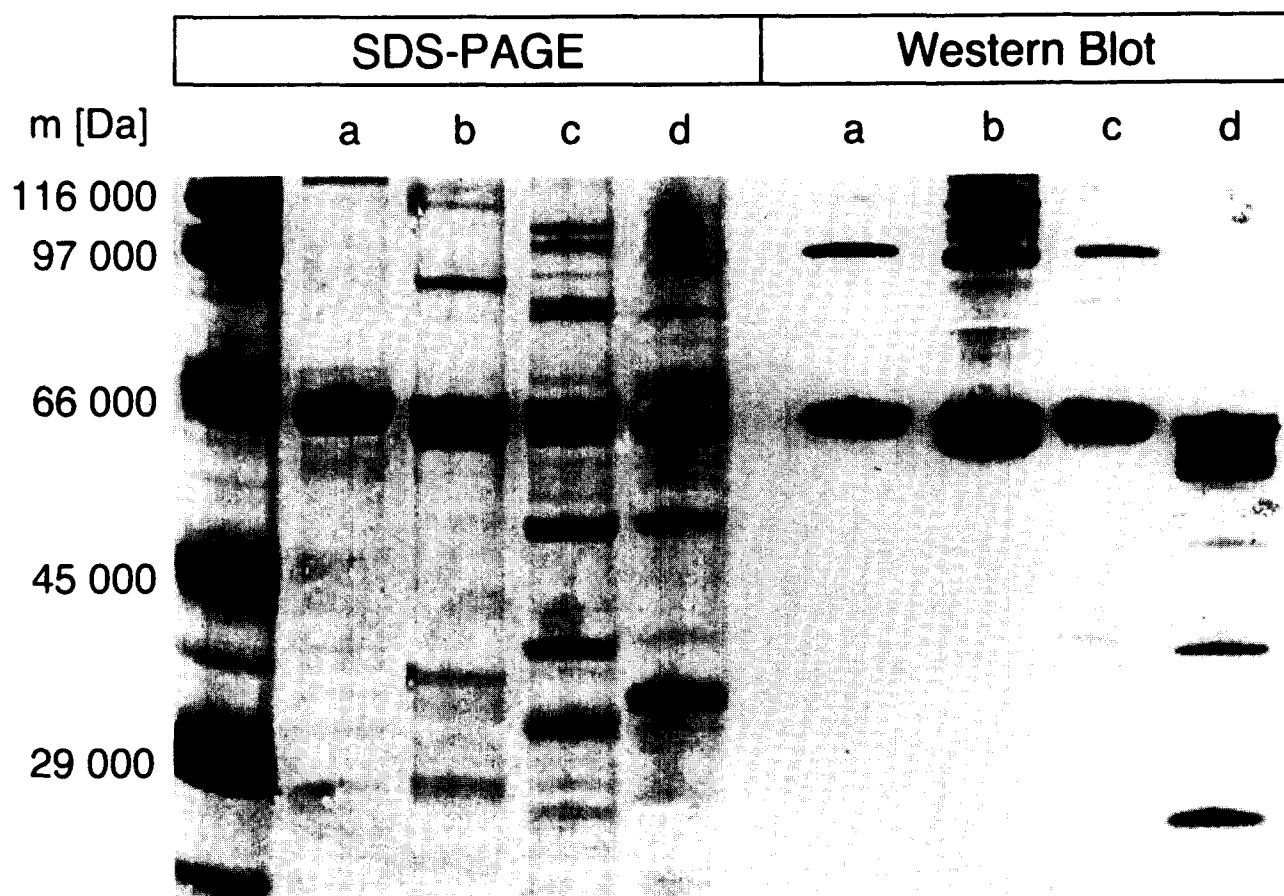


Fig. 2. SDS-PAGEs of purified recombinant complexes followed by Coomassie blue staining or Western blot analysis. Expression in *E. coli* was performed using the constructs indicated in Fig. 1. Lane a =  $\alpha$ -complex; lane b = native thermosome of *T. acidophilum*; lane c =  $\alpha$  +  $\beta$ -complex; lane d =  $\beta$ -complex. Molecular mass standards are given on the left side. Each lane contains 5  $\mu$ g of protein.

### 3. Results and discussion

#### 3.1. Expression and purification of the recombinant protein complexes

We have established a system for the efficient expression of the two subunits of the *Thermoplasma acidophilum* thermosome in *Escherichia coli*. The corresponding genes were subcloned into the expression vector pT7-7 yielding the construct pT7-7- $\alpha\beta$ . Both reading frames were preceded by an *E. coli* ribosomal binding site and organized in an operon under the control of the strong viral T7 promoter. After induction with IPTG, cells were harvested and a crude separation of cellular proteins was performed by SDS-PAGE, followed by Western blot analysis. We found both subunits highly expressed in the cytosol, although the  $\alpha$ -polypeptide was found in a slight excess over the  $\beta$ -polypeptide (data not shown). Expression of that operon using the vector pRSet 6a resulted in higher expression levels than using pT7-7, but did not change the ratio of the two polypeptides. The recombinant subunits were accessible for N-terminal protein sequencing, yielding amino acid sequences (M M T G for  $\alpha$ , and M I A Q for  $\beta$ ) which were identical to the sequences derived from the 5'-end of the genes [15].

The formation of high molecular mass complexes in the bacterial cytoplasm containing the two co-expressed proteins was indicated by size exclusion chromatography or non-denaturing

PAGE of cellular crude extract, both monitored by Western blot analysis. In order to characterize the composition of these complexes His-tags were introduced at the C-terminal end of either the  $\alpha$ -gene or the  $\beta$ -gene. These tags allowed the purification of the expressed proteins by a  $\text{Ni}^{2+}$ -chelate affinity column. Unfortunately, the binding efficiency of the polypeptides to the affinity column was rather low even when an unusually large column was used. We assume that, as in the GroEL-complex [17], the C-terminal ends of both subunits are directed towards the inner cavity of the toroid resulting in a poor accessibility for the column-bound  $\text{Ni}^{2+}$ -ion. Fractions containing sufficient amounts of the thermosome subunits, which eluted at imidazole concentrations of 300–500 mmol, were subsequently concentrated and applied to a size exclusion chromatography column. In high molecular mass fractions the formation of  $\alpha$  +  $\beta$ -complexes was indicated by the detection of both polypeptides in immunostained SDS-gels. These hetero-oligomeric complexes were reproducibly found when the His-tag was appended either to the  $\alpha$ - or  $\beta$ -subunit. Complexes, which had been purified via the His-tag of the  $\alpha$ -gene, apparently contained the  $\alpha$ -polypeptide in strong excess of the  $\beta$ -polypeptide. In contrast, complexes purified via the His-tag attached to the  $\beta$ -gene contained both subunits in nearly a 1:1 ratio (Fig. 2). The eluted protein fractions were found to be contaminated with small amounts of *E. coli* proteins as seen in the SDS-gels. Whether these

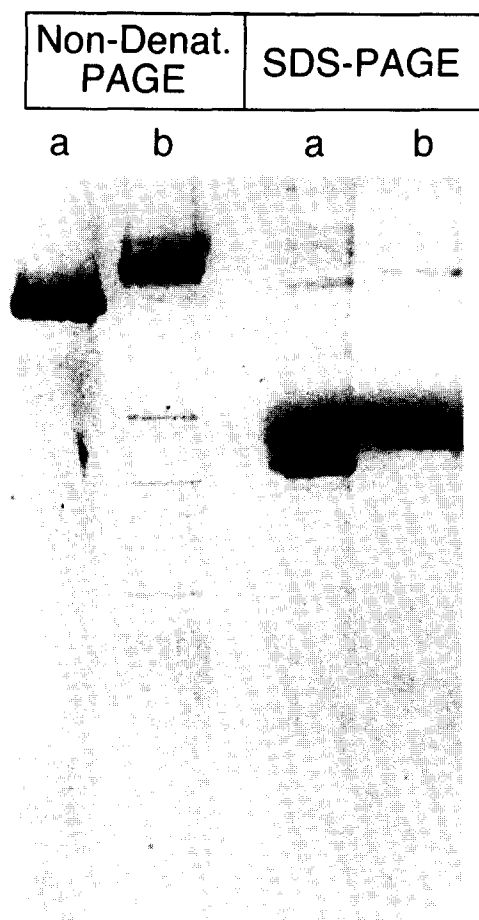


Fig. 3. Comparison of the  $\alpha$ -complex with the native thermosome by polyacrylamide gel electrophoresis. Protein bands were excised from the non-denaturing gel and analysed by SDS-PAGE. Lane a = native thermosome of *T. acidophilum*, lane b =  $\alpha$ -complex.

proteins are unspecific contaminations or polypeptides interacting specifically with the chaperonin-complexes in vivo remains unclear. One of the contaminants was identified as *E. coli* GroEL by immuno-staining using a sensitive antibody (Boehringer, Mannheim). Some minor bands were identified by immunostaining as proteolytic degradation products of the thermosome subunits. Upon longer storage of fractions containing  $\alpha + \beta$ -complexes at 4°C, an increased degradation especially of the  $\beta$ -subunit was seen. Interestingly, analysis of the expressed polypeptides by 2-dimensional PAGE (isoelectric focusing followed by SDS-PAGE, data not shown) resulted in a gel-pattern very similar to that of the native thermosome [15]. Both subunits were resolved into several spots of apparently identical mass but different pI indicating that they were posttranslationally modified also in the *E. coli* cytoplasm.

In order to find out whether both polypeptides were able to form thermosome-like particles separately, the genes were separately expressed in *E. coli*. The  $\alpha$ -gene possessing the C-terminal His-tag was subcloned into the expression vector pRSet 6a yielding pRSet 6a- $\alpha$ (6 His). The corresponding polypeptide was expressed in high levels and could be purified from the bacterial cytosol. In a denaturing polyacrylamide gel it migrated slightly higher than the *Thermoplasma*  $\alpha$ -subunit due to the additional

six histidine residues (Fig. 2). More than 50% of the expressed protein was found to be part of a high molecular weight complex as judged by size exclusion chromatography (data not shown). In non-denaturing PAGE this complex migrated more slowly than the native *Thermoplasma* thermosome yielding one high molecular weight band; sometimes a second faint band at a higher position was visible. When this gel region was excised and analysed by SDS-PAGE only the  $\alpha$ -polypeptide was detected (Fig. 3). The same result was obtained by SDS-PAGE analysis of purified  $\alpha$ -complexes (Fig. 2), proving that these complexes are indeed homo-oligomeric.

For separate expression of the  $\beta$ -subunit the vector pT7-5 was chosen since the corresponding gene contains several internal *Nde*I-sites. The protein was expressed in high levels in the *E. coli* cytoplasm and due to the appended His-tag it migrated above the *Thermoplasma*  $\beta$ -subunit in SDS-gels. The formation of  $\beta$ -complexes in the cytosol was detected by size exclusion chromatography (Fig. 4) and Western blot analysis. A more detailed biochemical characterization of the  $\beta$ -complex turned out to be difficult since it was apparently formed with lower efficiency and appeared to be less stable than the  $\alpha$ -complex. It dissociated during non-denaturing PAGE due to the pH of 8.8 in the gel and was prone to proteolytic degradation when stored at 4°C. It is unclear at this stage whether these observations simply reflect artefacts of the purification method, or are of relevance regarding the assembly mechanism of the thermosome in vivo.

In general, Superose 6 chromatograms of  $\alpha$ -,  $\beta$ - and  $\alpha + \beta$ -complexes were indistinguishable from each other and from the

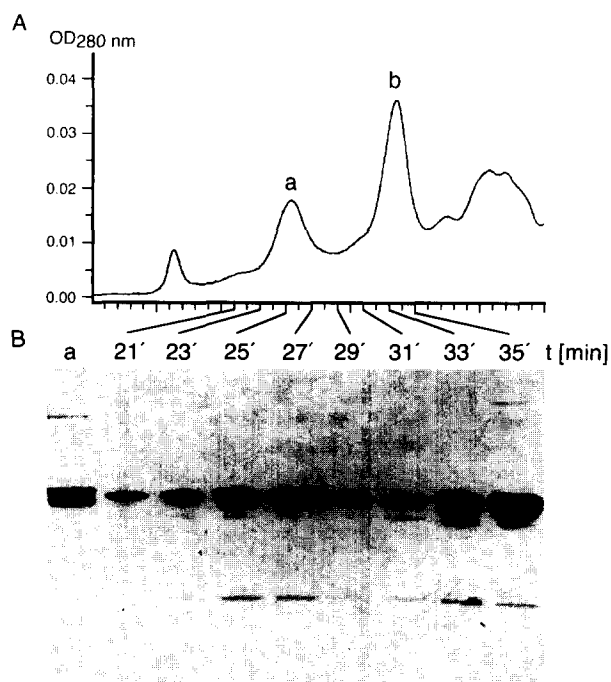


Fig. 4. Purification of the recombinant  $\beta$ -complex by size exclusion chromatography. Fractions eluted from the  $\text{Ni}^{2+}$ -chelate column (see section 2) were applied to a Superose 6 column resulting in separation of high molecular mass complexes from the copurified subunits. (A) Chromatogram of the Superose 6 column. Peak a contains high molecular mass complexes ( $M_r \sim 1 \times 10^6$ ), peak b = contains proteins of  $M_r \sim 60,000$ . (B) Western blot analysis of fractions eluted at the indicated times and separated by SDS-PAGE. Lane a = native thermosome of *T. acidophilum*.

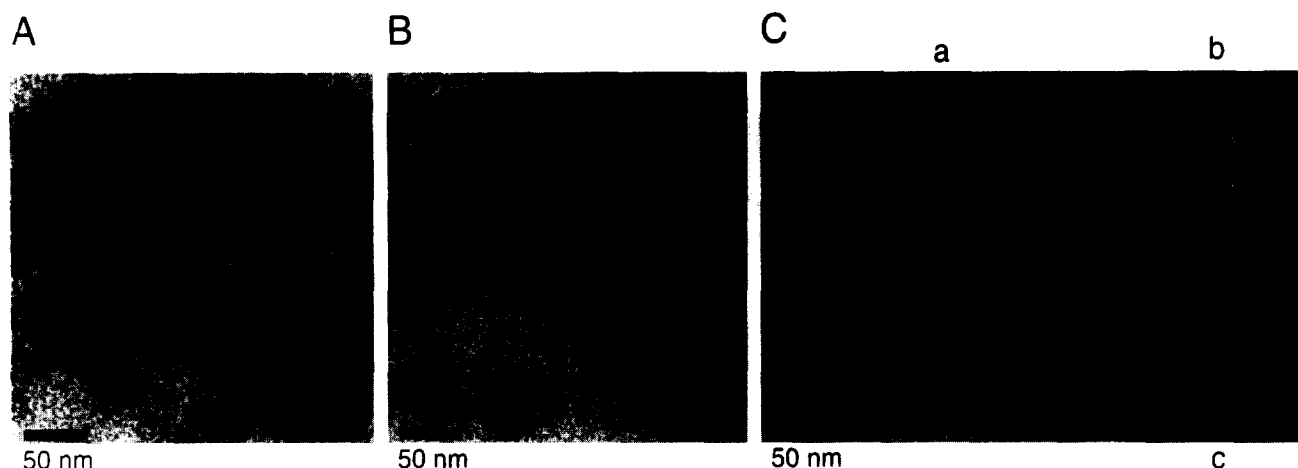


Fig. 5. Electron micrographs of negatively stained preparations containing the recombinant complexes as shown in Fig. 2. (A)  $\alpha + \beta$ -Complexes. Ring-shaped end-on views predominate but also some striated side-on views are visible. (B)  $\beta$ -Complexes. (C)  $\alpha$ -Complexes. Panel a = electron micrograph; panel b = average of 284 side-on views of the barrel-shaped complex; panel c = average of 968 end-on views revealing an eight-fold symmetric ring with a stain filled cavity at the center.

native thermosome regarding the respective retention times of the complex (~25 min) and of the free subunits (~33 min). No peak was detected at an elution time in between indicative of the formation of single octameric rings. For all three different complexes a weak ATPase activity at 60°C was detected colorimetrically using Malachite green as color reagent [12]. It is perhaps surprising that  $\alpha$  and  $\beta$  are able to form thermosome-like complexes on their own since both the native thermosome from *T. acidophilum* as well as the TF55-complex from *S. solfataricus* appear to be composed of two subunits in vivo [28]. In contrast to the *Thermoplasma* thermosome, the *S. solfataricus* complex, which shows a nine-fold rotational symmetry [14], is assumed to contain both subunits in a 2:1 ratio [28]. The subunit stoichiometry of the recombinant  $\alpha + \beta$ -complexes was difficult to determine since they could not be distinguished from homo-oligomeric  $\alpha$ - or  $\beta$ -complexes under the experimental conditions used. We cannot exclude that after co-expression of both subunits all three complexes ( $\alpha$ ,  $\beta$ ,  $\alpha + \beta$ ) co-exist in unknown ratios in the bacterial cytoplasm. We have indications that the  $\beta$ -complex is only formed if no  $\alpha$ -polypeptide is present. Consequently, since in our *E. coli* expression system the  $\alpha$ -polypeptide was more highly expressed than the  $\beta$ -polypeptide, the formation of homo-oligomeric  $\alpha$ -complexes may only occur after depletion of free  $\beta$ -polypeptides due to a preferred  $\alpha$ - $\beta$ -interaction.

### 3.2. Electron microscopy and image analysis

Transmission electron microscopy was used to examine the structure of the three different recombinant complexes. On electron micrographs of purified  $\alpha + \beta$ -complexes predominantly ring-shaped (end-on views) appeared, but also some striated complexes (side-on views) were observed (Fig. 5A). Averages of both orientations revealed the characteristic appearance of the thermosome particle [12,13]: pseudo eight-fold symmetric top views and barrel-shaped side views (data not shown). To examine the structure of the homo-oligomeric  $\alpha$ ,  $\beta$  complexes, electron micrographs of the corresponding preparations were subjected to a detailed image analysis. In the case

of the  $\alpha$ -subunit, end-on as well as side-on views were found (Fig. 5C). The average of 284 side-on views showed the typical appearance of the thermosome (Fig. 5C). Image processing including correspondence analysis (CA) was applied to 968 ring-shaped complexes in the end-on orientation. CA revealed the existence of only one type of symmetry within the dataset. The average showed clear eight-fold symmetry, and structure was indistinguishable at the present resolution from the native thermosome (Fig. 5C).

On electron micrographs of recombinant  $\beta$ -complexes predominantly end-on views were seen (Fig. 5B). Classification and averaging of 990 complexes using CA also revealed eight-fold symmetry, albeit less clearly. This is probably due to the poorer structural preservation of most of the complexes reflecting their lower stability (see above). After dialysis of fractions containing  $\beta$ -complexes against 100 mM Tris-HCl pH 8.8, ring-shaped particles could no longer be detected.

### 3.3. In vitro dissociation and reassembly

In order to test whether the thermosome subunits can self-assemble, we dissociated and reconstituted native and recombinant complexes in vitro (Fig. 6). The requirements for assembly were established using dissociated thermosomes isolated from *T. acidophilum*. As judged by both non-denaturing PAGE and electron microscopy the thermosome was stable at pH values between 4 and 11, but dissociated at pH 3 and lower. Due to its lower pI value, the  $\beta$ -subunit migrated almost two times faster than the  $\alpha$ -subunit in non-denaturing gels (Fig. 6A, lane b). We also examined under which conditions the thermosome subunits were able to reassemble into hexadecameric complexes (Fig. 6A). Dialysis of pH-dissociated thermosomes against near-neutral buffer led to the reappearance of thermosome-like complexes in non-denaturing gels or on electron micrographs (data not shown) only when both  $Mg^{2+}$  and ATP (Fig. 6A, lane c) or the non-hydrolyzable analogues ATP $\gamma$ S or AMPPNP (data not shown) were present in the dialysis buffer. When ATP was replaced by ADP or  $Mg^{2+}$  by  $K^+$ , complexes were detected neither on non-denaturing gels nor on electron micrographs

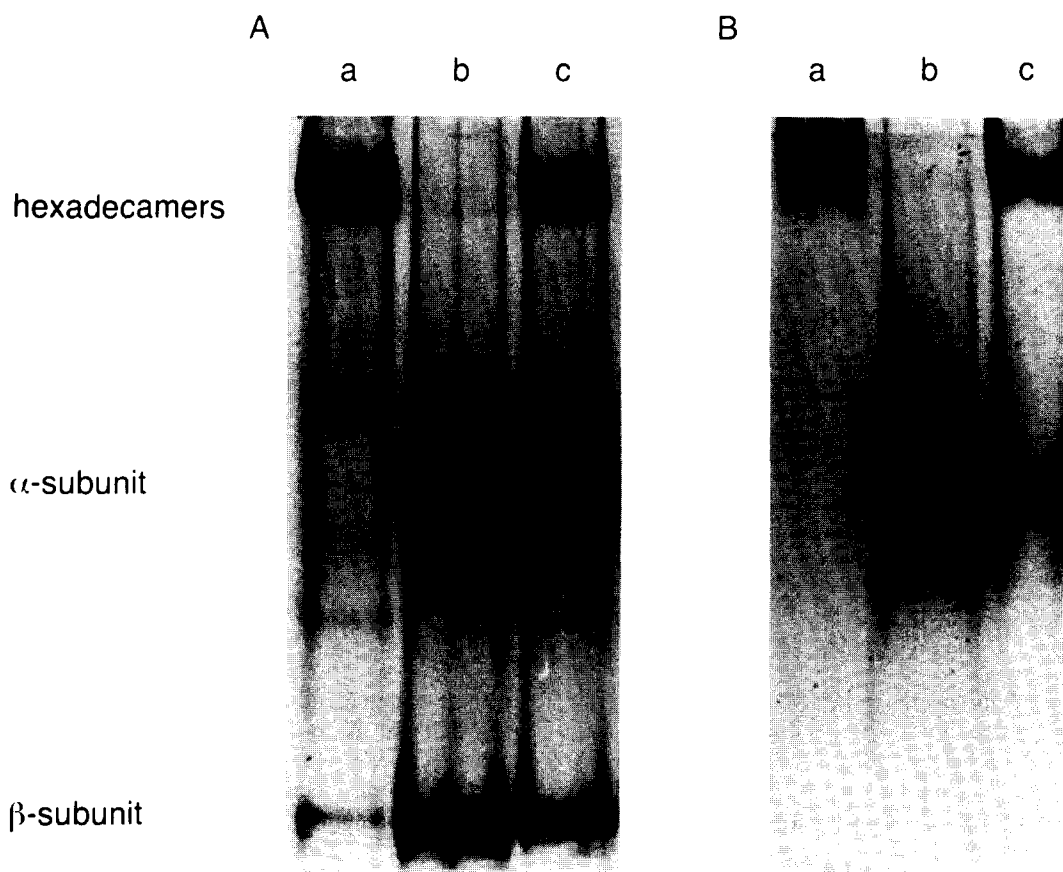


Fig. 6. Dissociation and in vitro reconstitution of the thermosome from *Thermoplasma acidophilum* (A) and of the recombinant  $\alpha$ -complex (B). Non-denaturing PAGE (3–12% polyacrylamide gradient in Tris-HCl, pH 6.8/8.8) was used to discriminate between hexadecameric complexes (top),  $\alpha$ -subunits (middle) and  $\beta$ -subunits (bottom). (A) Lane a = 10  $\mu$ g of thermosomes before dissociation; lane b = 10  $\mu$ g of thermosomes after 3 h incubation at pH 3; lane c = approximately 10  $\mu$ g of thermosomes after dissociation at pH 3 and subsequent dialysis against neutral buffer in the presence of  $Mg^{2+}$  and ATP. (B) As in (A), but using recombinant  $\alpha$ -complexes instead of the native thermosomes.

(data not shown). Consequently, only binding of Mg-ATP but not its hydrolysis seems to be necessary for the formation of hexadecameric complexes. However, this reassembly reaction was not quantitative and a significant amount of individual subunits was still visible in non-denaturing PAGE. After reassembly of the thermosome, two bands of high-molecular mass were frequently separated on non-denaturing gels. Separate excision of these gel regions and analysis by SDS-PAGE showed that the complexes corresponding to these two bands were both composed of approximately equal amounts of  $\alpha$ - and  $\beta$ -subunits (data not shown). On electron micrographs, the reassembled complexes appeared ring-shaped and were indistinguishable from the originally isolated thermosome.

Following the same protocol, also the recombinant  $\alpha$ -complex was dissociated and reassembled in vitro (Fig. 6B). In non-denaturing gels the band corresponding to the  $\alpha$ -complex (visible in lane a) disappeared after a 3 h incubation at pH 3 (lane b), indicating that the complex had dissociated completely into subunits. After dialysis of the subunits against neutral buffer containing ATP and  $Mg^{2+}$ , the high-molecular weight complex reformed (lane c). In accordance with this, ring-shaped top views of complexes were not detected on electron micrographs of the thermosome incubated at pH 3, but were clearly visible after dialysis (data not shown). The ability of the  $\alpha$ -subunits to assemble into hexadecameric complexes is in vari-

ance with observations made with TF55 from *S. solfataricus*. This complex was recently reported to reassemble in vitro only if both subunits were present [28].

Nevertheless, the thermosome and TF55 are similar in their dependence upon Mg-ATP for in vitro reassembly. As recently published,  $Mg^{2+}$  and ATP also promote the in vitro reassembly of several group I chaperonins after dissociation by urea [27]. However, also dissociation of these chaperonins is enhanced by adenine nucleotides [27]. This led to the proposal, that ATP facilitates an exchange between monomeric and oligomeric states of these chaperonins by inducing an assembly-competent conformation of the chaperonin molecule [27]. Because group I and group II chaperonins are related to each other in their equatorial, ATP-binding domain [15,16], a similar mechanism may also be responsible for the establishment of an equilibrium between thermosome subunits and complexes. However, because the thermosome concentration in vivo is not exactly known at present, the physiological significance of monomeric versus oligomeric forms of the thermosome remains an open question that deserves further examination.

**Acknowledgements:** The authors wish to thank Josef Kellermann for N-terminal sequencing of the polypeptides, Zdenka Cejka for her help with the pictures and Mary Kania for reading the manuscript. M.K. wishes to thank the Boehringer Ingelheim Foundation for a predoctoral fellowship.

## References

- [1] Ellis, R.J. and Van der Vies, S. (1991) *Annu. Rev. Biochem.* 321–348.
- [2] Hendrick, J.P. and Hartl, F.U. (1993) *Annu. Rev. Biochem.* 349–384.
- [3] Hartl, F.U. and Martin, J. (1995) *Curr. Opin. Struct. Biol.* 5, 92–102.
- [4] Horwich, A.L. and Willison, K.R. (1993) *Phil. Trans. R. Soc. Lond. B* 339, 313–325.
- [5] Gupta, R.S. (1995) *Mol. Microbiol.* 15, 1–11.
- [6] Kubota, H., Hynes, G. and Willison, K. (1995) *Eur. J. Biochem.* 230, 3–16.
- [7] Frydman, J., Nimmesgern, E., Erdjument, B.H., Wall, J.S., Tempst, P. and Hartl, F.U. (1992) *EMBO J.* 11, 4767–4778.
- [8] Kubota, H., Hynes, G., Carne, A., Ashworth, A. and Willison, K. (1994) *Curr. Biol.* 4, 89–99.
- [9] Phipps, B.M., Hoffmann, A., Stetter, K.O. and Baumeister, W. (1991) *EMBO J.* 10, 1711–1722.
- [10] Trent, J.D., Nimmesgern, E., Wall, J.S., Hartl, F.U. and Horwich, A.L. (1991) *Nature* 354, 490–493.
- [11] Rommelaere, H., Van, T.M., Gao, Y., Melki, R., Cowan, N.J., Vandekerckhove, J. and Ampe, C. (1993) *Proc. Natl. Acad. Sci. USA* 90, 11975–11979.
- [12] Waldmann, T., Nimmesgern, E., Nitsch, M., Peters, J., Pfeifer, G., Mueller, S., Kellermann, J., Engel, A., Hartl, F.U. and Baumeister, W. (1995) *Eur. J. Biochem.* 227, 848–856.
- [13] Phipps, B.M., Typke, D., Hegerl, R., Volker, S., Hoffmann, A., Stetter, K.O. and Baumeister, W. (1993) *Nature* 361, 475–477.
- [14] Marco, S., Urena, D., Carrascosa, J.L., Waldmann, T., Peters, J., Hegerl, R., Pfeifer, G., Sack-Kongehl, H. and Baumeister, W. (1994) *FEBS Lett.* 341, 152–155.
- [15] Waldmann, T., Lupas, A., Kellermann, J., Peters, J. and Baumeister, W. (1995) *Biol. Chem. Hoppe-Seyler* 376, 119–126.
- [16] Kim, S., Willison, K.R. and Horwich, A.L. (1994) *Trends Biochem. Sci.* 19, 543–548.
- [17] Braig, K., Orwinowski, Z., Hegde, R., Boisvert, D.C., Joachimiak, A., Horwich, A.L. and Sigler, P.B. (1994) *Nature* 370, 578–586.
- [18] Zwickl, P., Lottspeich, F. and Baumeister, W. (1992) *FEBS Lett.* 312, 157–60.
- [19] Zwickl, P., Kleinz, J. and Baumeister, W. (1994) *Struct. Biol.* 1, 765–770.
- [20] Löwe, J., Stock, D., Jap, B., Zwickl, P., Baumeister, W. and Huber, R. (1995) *Science* 268, 533–9.
- [21] Seemüller, E., Lupas, A., Stock, D., Löwe, J., Huber, R. and Baumeister, W. (1995) *Science* 268, 579–82.
- [22] Sambrook, J., Fritsch, E.F. and Maniatis, T. (1989) *Molecular Cloning. A Laboratory Manual*, 2nd edn., Cold Spring Harbour Laboratory Press, Cold Spring Harbour, NY, USA.
- [23] Tabor, S. and Richardson, C.C. (1985) *Proc. Natl. Acad. Sci. USA* 82, 1074–1078.
- [24] Schoepfer, R. (1993) *Gene* 124, 83–85.
- [25] Studier, F.W., Rosenberg, A.H., Dunn, J.J. and Dubendorf, J.W. (1990) *Methods Enzymol.* 185, 60–89.
- [26] Saxton, W.O., Pitt, T.J. and Horner, H. (1979), *Ultramicroscopy* 4, 343–354.
- [27] Lissin, N.M. (1995) *FEBS Lett.* 361, 55–60.
- [28] Knapp, S., Schmidt, K.I., Hebert, H., Bergman, T., Jörnval, H. and Ladenstein, R. (1994) *J. Mol. Biol.* 242, 397–407.